Proceedings of ASME Turbo Expo 2011
GT2011
June 6-10, 2011, Vancouver, British Columbia, Canada

GT2011-46838

AEROTHERMAL INVESTIGATIONS ON MIXING FLOW FIELD OF FILM COOLING WITH SWIRLING COOLANT FLOW

K. Takeishi[*] [†] , M. Komiyama , Y. Oda , Y. Egawa and T. Kitamura
Department of Mechanical Engineering,
Osaka University, Osaka Japan 565-0871
Email: takeishi@mech.eng.osaka-u.ac.jp

ABSTRACT

This paper describes the experimental results of a new film cooling method blowing through circular and shaped film cooling holes with swirling coolant flow.

The experiments have been conducted by using a scale-up model of a film cooling hole installed on the bottom surface of a low-speed wind tunnel. Swirling motion of film coolant was induced inside a hexagonal plenum by two slant impingement jets, which are inclined at α degree toward the vertical direction and installed in a staggered position. The two impingement jets generate swirling flows inside the plenum, and this swirling flow enters into a film cooling hole keeping the angular momentum until the exit of the film cooling hole. The slant angle of the impingement jets was changed as $\alpha = 0^\circ$, 10°, 20°, 30° in their wind tunnel tests.

The film cooling effectiveness on the flat wall was measured by using pressure sensitive paint (PSP) technique. In addition, the spatial distribution of non-dimensional concentration (or temperature) and flow field were measured by laser induced fluorescence (LIF) and particle image velocimetry (PIV), respectively.

In case of the circular film cooling hole, the coolant jet penetration into mainstream is suppressed by swirling motion of the coolant. As a result, though the coolant jet is deflected in the pitch direction, the film cooling effectiveness distribution on the wall keeps higher value behind the cooling hole over a long range. Additionally, kidney vortex structure disappeared. For the shaped cooling hole, the coolant jet spreads wider in spanwise direction at the downstream. Thus, the pitch averaged film cooling effectiveness at the downstream was 50% higher than that of the non-swirling case.

[*]Address all correspondence to this author, [†]ASME Member

INTRODUCTION

Gas turbines are used for aircraft propulsion and land-based power generation. Developments in turbine cooling technology play a crucial role in increasing the thermal efficiency and power output of advanced gas turbines. Gas turbine's blades and vanes are cooled externally by film cooling in high temperature gas turbines. It is achieved by injecting relatively cooler air from the internal coolant passages out of the blade surface in order to form a protective layer between the blade surface and hot gas-path flow. The interaction between film-cooling air and mainstream, which is representative of film cooling, forms a shear layer that leads to mixing and a decay of the film cooling performance along a blade surface. It is important to improve the film cooling effectiveness by minimizing the film cooling air flow rate.

The cooling air blowing through an inclined circular hole penetrates into mainstream and generates kidney vortex structure by the interaction between mainstream and film cooling jet. The downwash of hot mainstream gas catches the hot gas under the film cooling air jet and clearly decreases the film cooling effectiveness on turbine blade surfaces. Shaped film cooling is one of the most attractive inventions by incorporation of exit shaping to the film holes, which results in lower momentum coolant injection jets with greater surface coverage.

There have been many studies on film cooling. A review paper by Goldstein [1] summarized early works in this area and Bogard and Thole [2] reviewed the latest one. Early investigations on film cooling were about the flows blowing through inclined discrete holes, including Eriksen and Goldstein [3] and Bernsdorf et al. [4]. The efforts to improve film cooling efficiency by adopting film cooling holes with expanded exits have been made experimentally by Goldstein and Eckert [5], Bell et al. [6], Takeishi and Aoki. [7] and Yu et al. [8]. An excellent summary paper on shaped film cooling was published by Bunker [9].

Several new ideas to control anti-kidney vortex structure have been presented. Kusterer et al. [10] investigated two film cooling arrangement with different compound angles, and Heidmann [11] proposed additional cooling air jets in a circular film cooling hole to control and to crash the kidney type vortex. Rigby and Heidmann [12] placed a delta vortex generator downstream of the ejection hole and found that the vortex generator was very effective at producing an anti-kidney vortex pair. The resulting anti-kidney vortex pair caused coolant to be pushed toward the wall and spread out along the wall. Ely and Jubran [13] have studied a “sister hole” arrangement which leads to an increased film cooling efficiency due to the established vortex structure.

In this paper a new film cooling scheme to cool the endwall of a first vane for high temperature industrial gas turbines is proposed. It is built with a hexagonal shell structure with two inclined impingement nozzles on the cover plate of the hexagonal shell and the swirling coolant flow generated by the inclined impingement nozzles will blow through film cooling hole on the endwall. This concept can control the film cooling flow rate and blowing ratio to optimize the film cooling effectiveness on the endwall.

The effect of the swirling motion to the film cooling is also important in the actual turbine blades and vanes. Because, in modern air cooled turbine vanes and blades, impingement cooling and serpentine flow passage with turbulent promoter are adopted to cool the airfoil and endwall internally. Such cooling method utilized vortex motion of cooling air to improve the heat transfer coefficient. And film cooling air is usually ejected from these air sources which still keeps weak or strong vortex. The vortex motion in the bleeding film cooling air may improve the film cooling effectiveness if the strength of the vorticity matches the film cooling condition [14]. In addition to the utilization of the vortex motion in the internal cooling air flow, invention of a new cooling method utilizing an actively generated vortex motion in the film cooling flow will be most important to improve film cooling effectiveness in high temperature gas turbine’s vane and blade. But, there are very few open literatures available which treat the film cooling with swirling flow. Kuya et al. [15] studied the effect of swirled film cooling air on film cooling effectiveness by using a twisted tape in a circular cooling hole and found an improvement of film cooling effectiveness with swirling coolant flow. But, there was no quantitative description and experimental results to understand the mechanism of the film cooling with swirling flow.

Recently, Takeishi et al. [16] have developed a measurement system to obtain instantaneous and time-averaged mixing flow fields of film cooling air and mainstream using the Laser-Induced Fluorescence (LIF) method, and demonstrated that it can be a strong tool to investigate the mechanism of mixing process in film cooling in view of instantaneous fields.

In this study, a swirling motion of coolant flows was realized by two staggered-facing impinging jets with a slant angle, which give angular momentum to the coolant air inside the plenum chamber. To examine the effect of the swirl on the film cooling effectiveness, the film cooling effectiveness on the wall of a low speed wind tunnel was measured by pressure sensitive paint (PSP) technique for circular and shaped holes, and the spatial distribution of the film cooling effectiveness and flow field were measured by laser induced fluorescence (LIF) and particle image velocimetry (PIV), respectively.

EXPERIMENTAL APPARATUS AND METHOD

Wind tunnel and film cooling models

The present experiment has been conducted using a scale-up model of film cooling holes installed on the bottom surface of a low-speed wind tunnel in order to allow detailed probing of flow features. The wind tunnel is an open-circuit and subsonic flow can be produced through an inlet nozzle with a 9:1 contraction ratio as shown in Figure 1. At the inlet of the nozzle section, there were a honeycomb and meshed screens. Therefore, the airflow has low turbulence intensity and uniform velocity profile at the entrance of the test section. The test section is 300 mm wide, 300 mm in height, and 1950 mm long. The air speed inside the test section can be varied from 0 to 40 m/s. For the free-stream velocity of 20 m/s, the flow at the test section shows excellent spatial uniformity, with free stream turbulence intensity less than 0.36%. A film cooling hole is located 950 mm downstream from the exit of the contraction section.

Figure 2 shows the geometry of film cooling holes, whose shapes are similar to those used by Takeishi and Aoki [7]. It was made of urethane resin (Sanmodur MS) with low thermal conductivity of k = 0.196 W/(mK) to reinforce adiabatic condition. The guide channel to the exit of the film cooling hole was inclined at 30 degree toward the main flow direction. The shaped hole is composed of a round tube section with a uniformly and symmetrically expanded exit in the end, where a fan-shaped diffuser exists with 15-degree divergence angles on both lateral sides. The diameter of the guide channel, d, was 5 mm. Coordinate axes and the origins were also shown in Figure

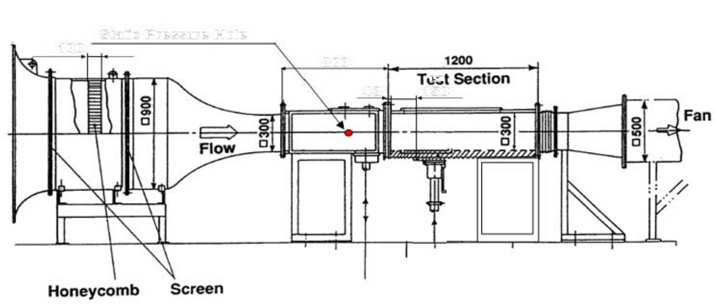

Figure 1 Low speed wind tunnel test facility

2. In order to compensate the viscous dissipation of the angular momentum (or velocity) inside the guide channel, the wall thickness of the shaped film cooling model is half of that of circular film cooling model to maintain effectual angular momentum (or velocity) at the exit of shaped hole, of which expanded exit area leads to smaller angular velocity even if the effective swirl number at the hole exit is the same as that of the circular hole.

Swirling coolant flow is made in a cavity that is located in a plenum before entering into a film cooling hole. A schematic view of the cooling structure is shown in Figure 3. The cross-section shape of the cavity is hexagonal, because it can be set successively without void space in real applications. It has two impingement jet holes, and they are inclined at α degree toward the vertical direction. Two impingement jets generate swirling flows inside the cavity, and this swirling flow enters into a film cooling hole keeping the angular momentum. Swirl number S at the exit of the film cooling hole was calculated by using measured w and u with PIV method for circular hole. Swirl number S is defined by Eq. (1)

$$S = \frac{G_a}{G_t R} \tag{1}$$

where R is radius of the flow channel.

G_a and G_t are angular momentum mass flow rate and translation momentum mass flow rate respectively, and defined by the following equations.

$$G_a = \int_0^R (wr)(\rho u)(2\pi r)dr \tag{2}$$

$$G_t = \int_0^R (\rho u^2 + p)(2\pi r)dr \tag{3}$$

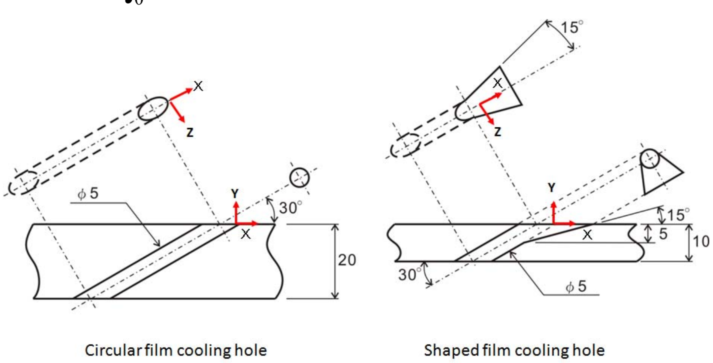

Figure 2 Geometries of film cooling holes

Table 1: Experimental Conditions

Mainstream velocity [m/s]	20
Turbulence intensity [%]	0.36
Boundary layer thickness [mm]	25
Blowing ratio	0.5-2.0
Film cooling hole diameter [mm]	5
Impingement jet angle [degree]	0, 10, 20, 30

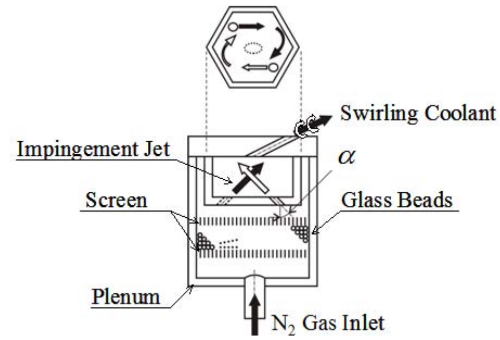

Figure 3 Structure of film cooling with swirling flow

In the present study, the two impingement jets angle was changed as θ = 0º, 10º, 20º, 30º, and the corresponding swirl number was estimated at S = 0, 0.0289, 0.116, 0.168, by PIV method at the exit plane in the circular hole respectively. The experimental conditions are shown in Table 1.

PSP methods

In this study, PSP was used to measure the film cooling effectiveness distribution on the wall. PSP is an optical pressure sensor. It uses a special pigment that changes its luminescence intensity by the reaction with oxygen molecules. The change of luminescence intensity is caused by optical quenching of the pigment by oxygen molecules. Therefore, we can measure a change of the concentration of oxygen by the luminescence intensity of the pigment. Before starting the film cooling tests, calibration tests have been conducted by using a psp painted plate whose temperature is controlled by Joule heating in a closed cavity. The luminescence intensity from the PSP was measured for the various combinations of the concentration of oxygen in the cavity and the temperature of the PSP painted plate, and we got calibration curves to estimate the concentration of oxygen from the measured luminescence intensity and temperature. By using air (concentration of oxygen is 21 %) for mainstream and nitrogen (concentration of oxygen is 0 %) for film cooling jet, the concentration distribution of oxygen, which is determined by the mixing of mainstream (air) and coolant (nitrogen), can be measured on the wall downstream of the film cooling hole. The film cooling effectiveness was defined by the following equation:

$$\eta = \frac{T_\infty - T_f}{T_\infty - T_c} \tag{4}$$

where T_∞ and T_c are temperatures of mainstream and coolant in the plenum respectively; T_f is the adiabatic wall temperature. Then, using an analogy between heat/mass transfers, Eq. (4) is changed to Eq. (5).

$$\eta = \frac{C_\infty - C_f}{C_\infty - C_c} \tag{5}$$

where C_∞ and C_c are concentration of the oxygen in mainstream and plenum chamber respectively; C_w is the concentration of the oxygen in the film cooling air just above the wall.

The blowing ratio, which is defined as Eq. (6) was controlled by changing the film cooling air flow rate..

$$M = \frac{\rho_c u_c}{\rho_\infty u_\infty} \tag{6}$$

The wall of the wind tunnel is painted with PSP (ISSI PtTfPP FIB-UF405). Nitrogen gas for film cooling is supplied from nitrogen gas tank. Thus, C_c and C_∞ are 0% and 21%, respectively, and C_w is measured by the following method. LED light sources with wave length 405 nm were used as an excitation light source. The images were taken with a CCD camera (Hamamatsu photonics C9440-05C 1344×1024 pixels, 12bit) located at the opposite side of PSP painted wall. Here, the light except phosphorescence (wave length 650 nm) was cut by a band pass filter. The images were digitally stored on hard disks using the acquisition software HIPIC 8.30. The three images, a background image, an image when wind tunnel was pausing and an image when wind tunnel was operating, were captured. 20 images were captured in each case, and they were averaged. PSP's luminescence intensity is affected by its temperature and hence the temperature of the wall during the experimentation was monitored by K-type thermocouples. In the plenum, there were screen and glass beads to prevent direct entrance of the supplied air into the impingement cooling holes.

Laser Induced Fluorescence (LIF)

LIF is a method for measuring concentration in gaseous flows. The advantages of LIF consist in being non-intrusive, instantaneous, and having high intensity of the fluorescence. In addition, LIF can realize high spatial resolution for the tracer concentration field. The flow is illuminated by a laser sheet of a wavelength that is tuned to excite a specific absorption transition of a molecular tracer, which is added for this purpose. A fraction of the molecules in the lower energy level absorbs the incident light and is excited to a higher energy state. When the excited state returns to the states with lower energy, fluorescence light is emitted with a different wavelength from that of the incident light. Thus, the fluorescence light from the tracer is extracted easily from the scattered light by using an interference filter.

If the thermal diffusivity of air and the mass diffusivity of a tracer are close, the thermal diffusion can be replaced by mass transfer based on heat/mass transfer analogy. Thus, non-dimensional temperature θ can be replaced by equation (7).

$$\theta = \frac{T_\infty - T}{T_\infty - T_c} = \frac{C_\infty - C}{C_\infty - C_c} \tag{7}$$

Lozano et al. [17] showed that acetone is known as one of the tracers for concentration measurements in gaseous flows by LIF, and the ratio between acetone vapor's mass diffusion coefficient through air, D, and the thermal diffusivity of standard air, a, is about one to two (D = 11.2 mm^2/s, a = 22.3 mm^2/s) [18]. This is close enough to apply the heat/mass transfer analogy. In addition, acetone LIF is known to show good linearity with respect to the partial pressure of acetone in the atmospheric pressure gas. Thus, we use acetone as the tracer to measure spatial non-dimensional concentration distribution θ by LIF method.

The Nd:YAG laser of wavelength 266 nm was used as excitation laser light. The beam was expanded to a sheet of 25 mm width and 1 mm thickness with four cylindrical lenses, passing through the test section, as shown in Figure 4 [16]. The saturated acetone vapor in air is produced by bubbling the air in bottles containing acetone liquid. In order to obtain optimal acetone vapor concentration, dry air is mixed with air saturated with acetone vapor in a scheduled ratio [19] [20] [21].

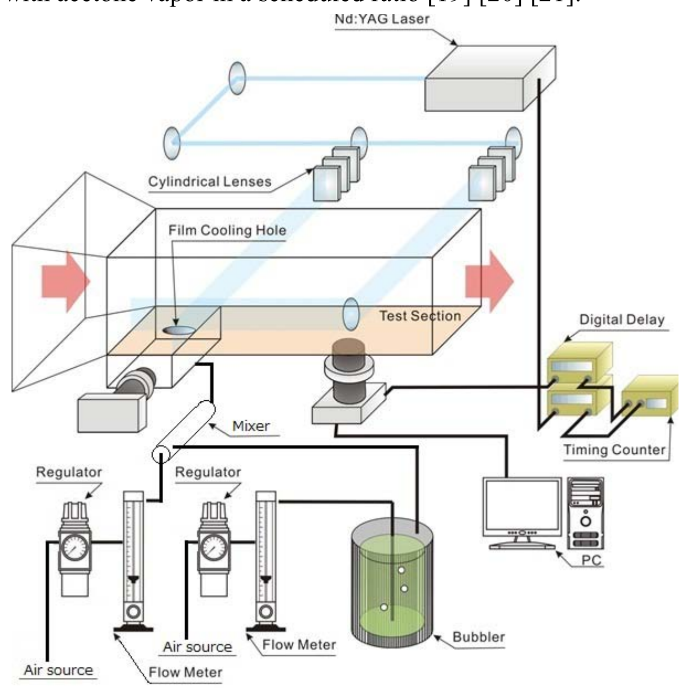

Figure 4 Schematic layout of acetone LIF method

Particle Image Velocimetry (PIV)

PIV was used to capture instantaneous velocity fields. The mainstream and the secondary flow blowing through film cooling holes contains fine particles of olive oil as a tracer, which are about 1μm in diameter. The particles of olive oil are generated by bubbling the compressed air into a pool of olive oil through a Raskin nozzle in a pressure vessel. In the vessel, air bubbles burst at the olive-oil/air interface and about 1μm olive oil particles are released into the air. A dual-pulsed Nd:YAG laser, of wavelength 532 nm, was employed to illuminate the tracers. Three cylindrical lenses were used to form a laser sheet. The laser sheet was guided by a mirror located downstream to illuminate the test window. The particle pattern formed by the light reflected on the particle surfaces were taken with a CCD camera located at the side of the test section. To reduce the effect of reflection from the bottom surface, a background image for each pulse is subtracted from each frame to eliminate the effect of laser light reflection. The pairs of captured images were processed by a recursive local-correlation method to obtain velocity vector fields.

RESULTS AND DISSCUSSION

Adiabatic film cooling effectiveness

Figures 5 and 6 show the adiabatic film cooling effectiveness contours of a circular hole at M = 0.5 and 1.0 measured by PSP method with impingement nozzle angle $\alpha = 0^{\circ}$ to 30º respectively. In the case of the blowing ratio of M = 0.5, the surface is covered with film cooling air because the penetration of the film jet into the mainstream is weak and the film jet is bent to the wall direction by the mainstream. The film cooling effectiveness decreased firstly at $\alpha = 10^{\circ}$ and improved a little with an increase of impingement nozzle angle from 10º

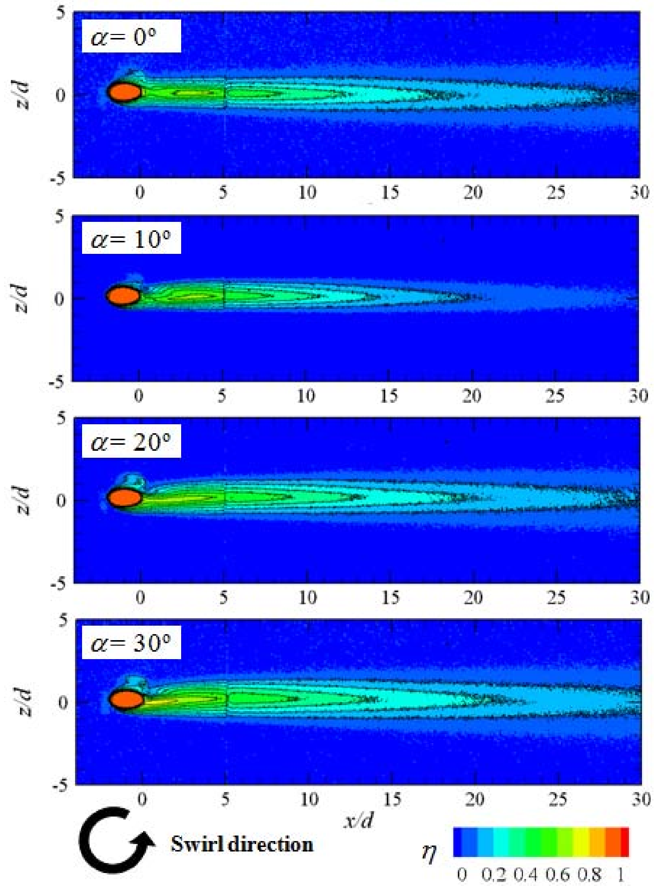

Figure 5 Film cooling effectiveness contours of circular hole with blowing ratio M = 0.5

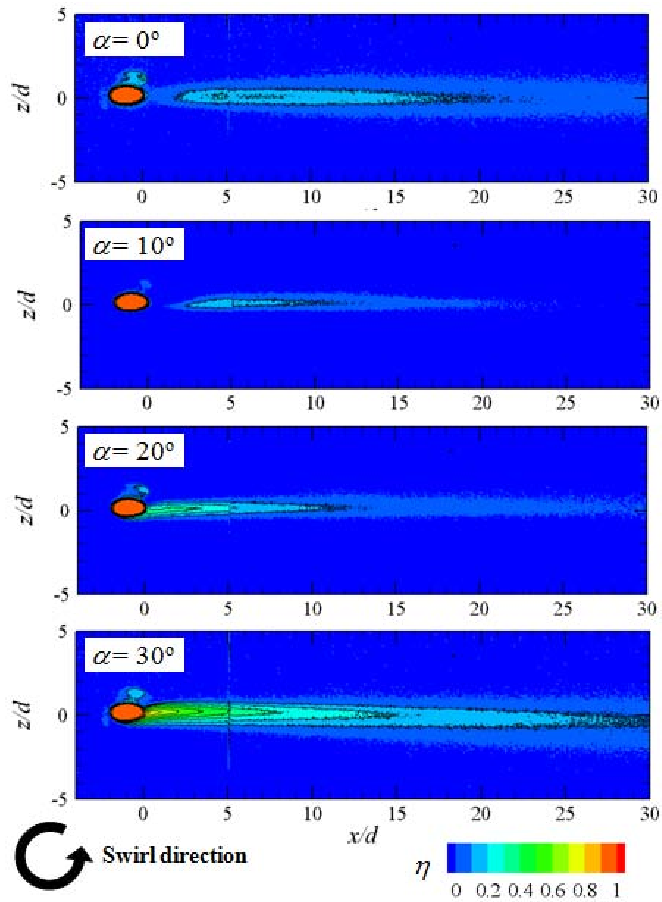

Figure 6 Film cooling effectiveness contours of circular hole with blowing ratio M = 1.0

to 30º as shown in Figure 5. In the case of flow with $\alpha = 0^{\circ}$ at M = 1.0 shown in Figure 6, the film cooling effectiveness just downstream the film cooling hole shows very low value. The reason of this low value is the lift off effect of film cooling jet into the main stream. At the downstream, the film cooling air is bent to the wall direction by the mainstream and reattaches on the surface near x/d = 3 and the film cooling effectiveness recovers to about 0.2. At $\alpha = 10^{\circ}$, the area covered by film cooling air is decreased. A weak swirl motion in the film cooling flow may deform symmetric kidney shape to asymmetric one and the downwash of hot mainstream gas may capture the hot gas under the film cooling air jet and decreases the film cooling effectiveness. However, further increase of swirl number suppressed the penetration of the film cooling jet and high film cooling effective area appeared in the vicinity of the film cooling hole exit. At $\alpha = 30^{\circ}$, the highest film cooling effectiveness of about 0.6 is marked just downstream the film cooling hole exit. The result indicates that the penetration of the film cooling jet into the main stream was suppressed strongly by swirling motion of the film cooling air. It appeared that the centre line of the cooling jet flow was deflected to the negative z direction at the film cooling hole exit. Considering about the relation between the swirling direction of the film cooling jet and the deflected direction of the film jet, we found that the cooling jet moved to the direction where the swirling velocity component in the x direction is positive. Figures 7 and 8 show the adiabatic film cooling effectiveness, which is laterally averaged over -3 < z/d < 3, with regard to the swirl number and x/d, respectively. Small data gaps at x/d = 5 in Figure 8 come from an actual small gap in the test section due to the removable mechanism of the film cooling test model mounted to the bottom surface of the low speed wind tunnel. The effect of the investigated swirl number on the circular hole film cooling effectiveness at blowing ratio M = 0.5 and 1.0 is clear to improve the film cooling effectiveness. Figure 8 shows that swirling coolant at α = 30º improved the averaged film cooling effectiveness about 50% at x/d = 10 and 100% or more compared to that of α = 0º at far downstream of x/d = 20. It appeared from Figure 8 that swirling coolant flow is very effective to improve the film cooling effectiveness for circular hole by suppressing both the penetration of cooling jet into mainstream and the generation of kidney vortex structure.

Figures 9 and 10 show the adiabatic film cooling

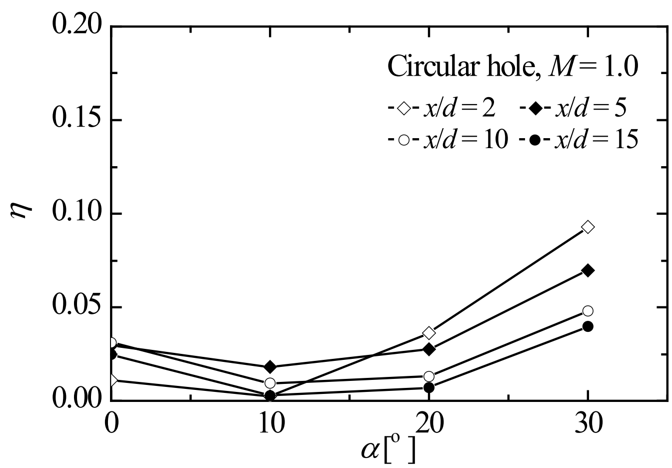

Figure 7 Lateral average effectiveness versus impingement jet angle (circular hole at M=1.0)

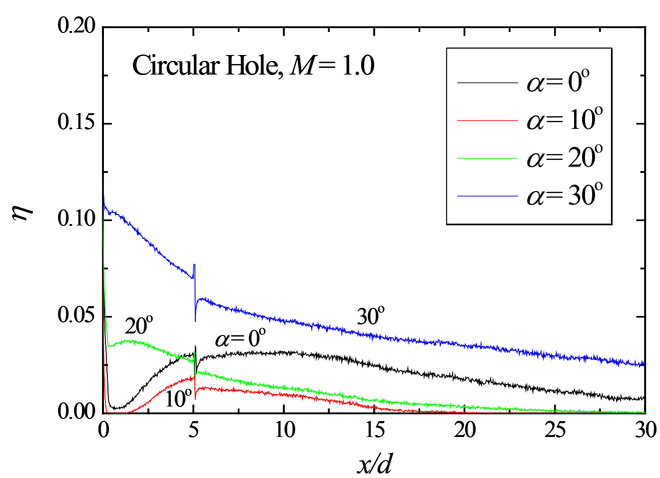

Figure 8 Spanwise-averaged film cooling effectiveness

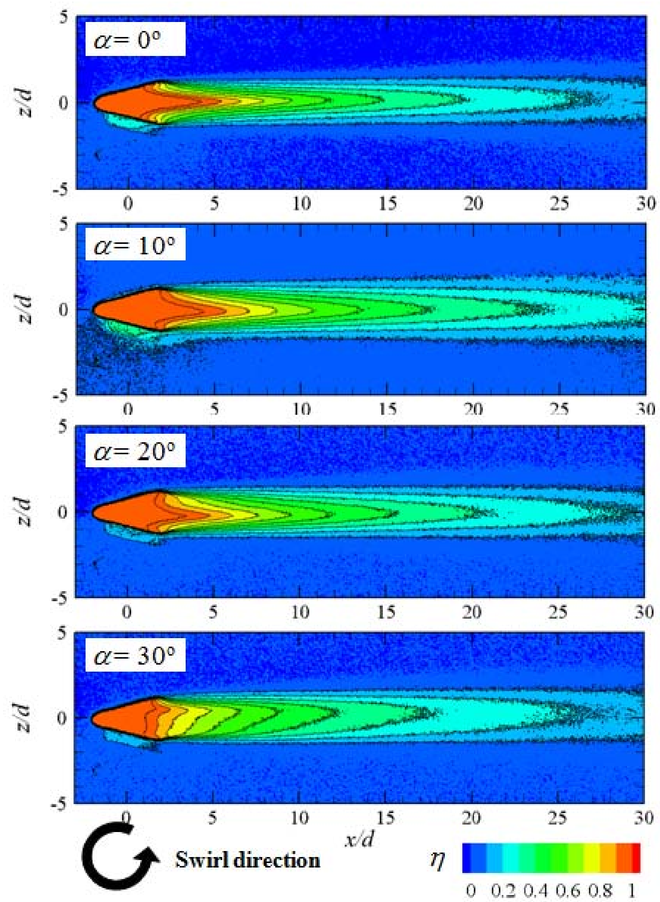

Figure 9 Film cooling effectiveness contours of shaped hole at blowing ratio M = 0.5

effectiveness contours of a shaped film cooling hole at M = 0.5 and 1.0 respectively measured by PSP method with α = 0º to 30º. Figures 9 and 10 show that the film cooling jet blowing through a shaped cooling hole spreads wider both lateral direction and long distance. Shaped film cooling attains higher film cooling effectiveness than circular hole by incorporation of exit shaping to the film holes, which results in lower momentum coolant injection with greater surface coverage. It appeared that the film cooling effectiveness reached the maximum value at α = 10 and decreased with increasing impingement inclined angle α. The next two figures, Figures 11 and 12 show quantitatively what the contour plots of Figure 10 shows pictorially. These figures shows the laterally averaged values of the adiabatic film cooling effectiveness at M = 1.0 with regard to the swirl number α = 0º to 30º and x/d, respectively. The effect of the investigated swirl number on the shaped hole film cooling effectiveness at the blowing ratio M = 1.0 is clear that the film cooling effectiveness attains the maximum value at α = 10º and it decreases with increasing impingement inclined angle α. The reason is clear from the film cooling effectiveness contour at α = 30º in Figure 10. This contour clearly shows that the positive

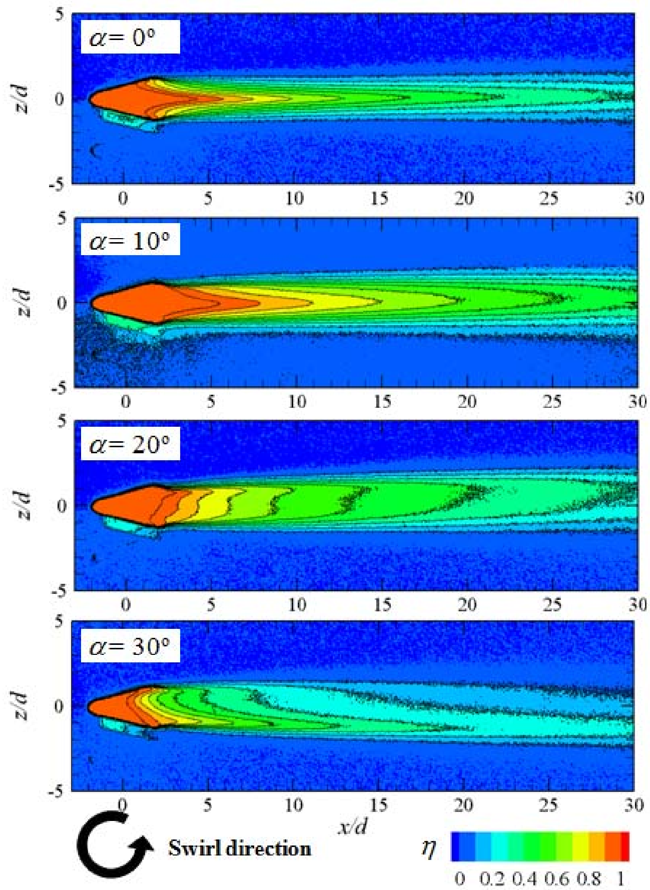

Figure 10 Film cooling effectiveness contours of shaped hole blowing ratio M = 1.0

z part of the film cooling layer is rolled up by the strong swirling motion of the film cooling air jet. Figure 12 shows that swirling coolant also improved the averaged film cooling effectiveness of shaped film cooling hole about 100% at far downstream of x/d = 10. There should be an optimum combination of shaped film cooling hole geometry and swirl number. In this case of the geometry shown in Figure 2 the averaged film cooling effectiveness achieves the maximum at α = 30º.

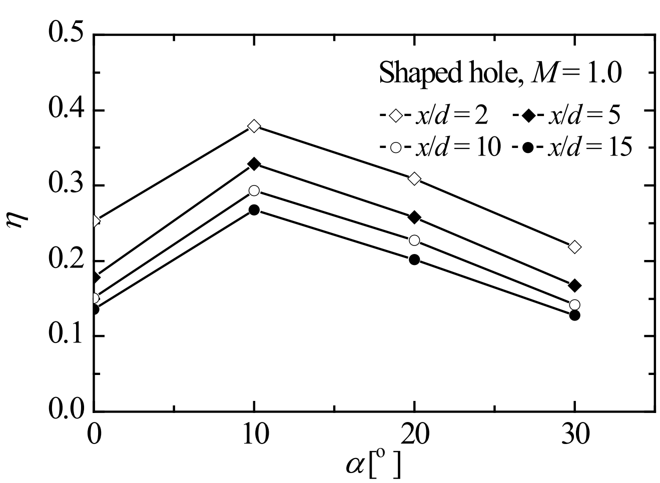

Figure 11 Lateral average effectiveness versus impingement jet angle (shaped hole at M=1.0)

Figure 13 shows the same plot as Figure 12, but for M = 2. It appeared that the same tendency of film cooling effectiveness with M = 1.0 was obtained at M = 2.0.

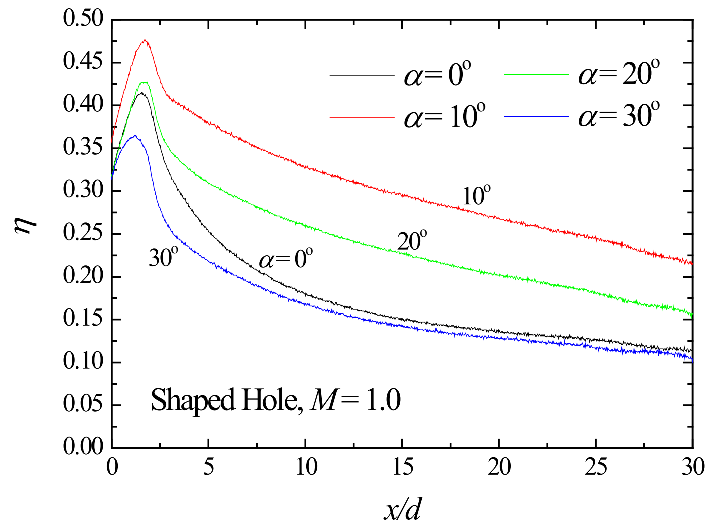

Figure 12 Spanwise-averaged film effectiveness at M=1.0

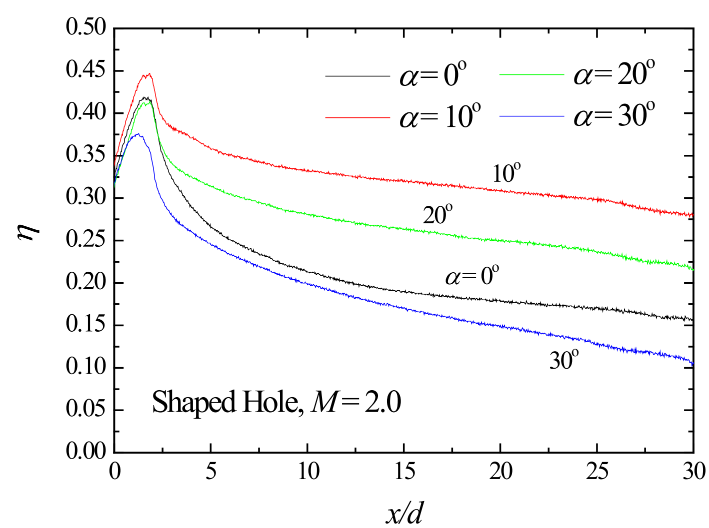

Figure 13 Spanwise-averaged film effectiveness at M=2.0

Spatial non-dimensional concentration/temperature distribution

Figures 14 and 15 show the time-averaged film cooling effectiveness distribution at z/d = 0 and the cross sections at selected locations obtained by acetone LIF near the exit of a circular hole, for blowing ratios of M = 1.0. Figure 15 is a view from upstream. It appeared from Figure 14 that the penetration of the film cooling jet into mainstream was suppressed by swirling coolant flow and attained higher film cooling effectiveness compared to the non-swirling coolant flow case. Figure 15 clearly shows the generation of kidney vortex structure at α = 0º, but kidney vortex is destructed at α = 30º to make part of the film cooling air adhere on the wall. Comparison of the measured LIF results at α = 0º and α = 30º in Figure 15 show that the swirling film cooling flow interacted with mainstream and suppressed the lift off of the film cooling jet and the formation of kidney vortex, and these results lead the coolant adhesion on the wall.

Figures 16 and 17 show the time-averaged film cooling effectiveness distribution at z/d = 0 and the cross sections at selected locations obtained by acetone LIF near the exit of a shaped hole, for blowing ratios of M = 1.0. It is clear from Figure 17 that the swirling film cooling flow at low swirl number α = 10º suppressed the penetration of the film cooling air into the mainstream and spreads the film cooling air in spanwise direction. As a result, the swirling film cooling air covers wide area on the wall, and attains the highest film cooling effectiveness as it is clear from Figure 11. But

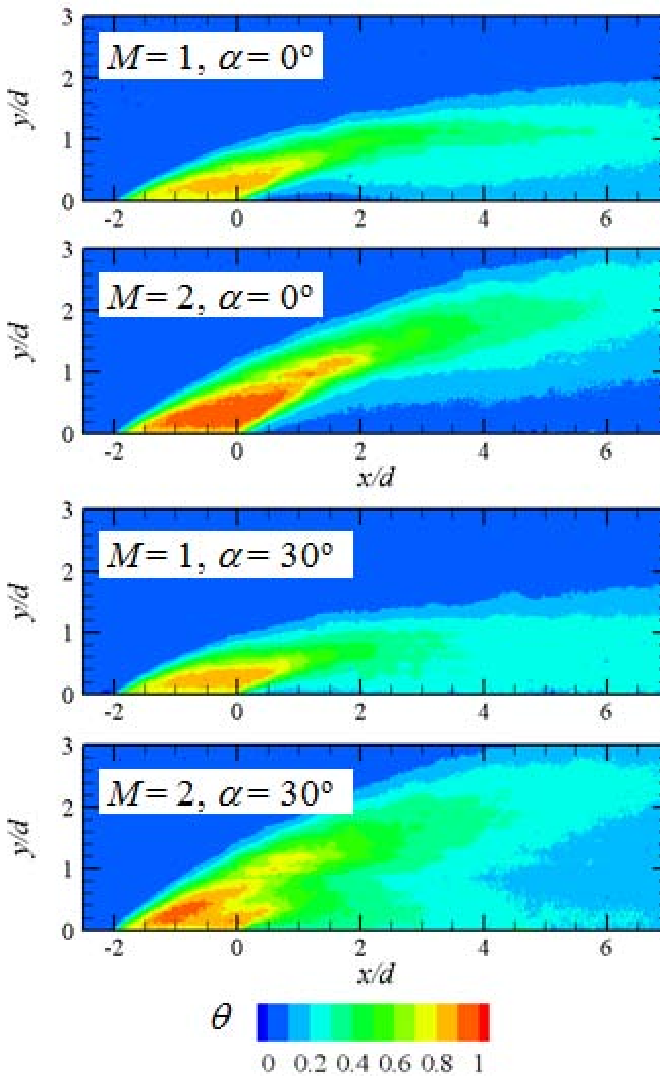

Figure 14 Spatial non-dimensional concentration contours (circular hole at *z/d*=0 section)

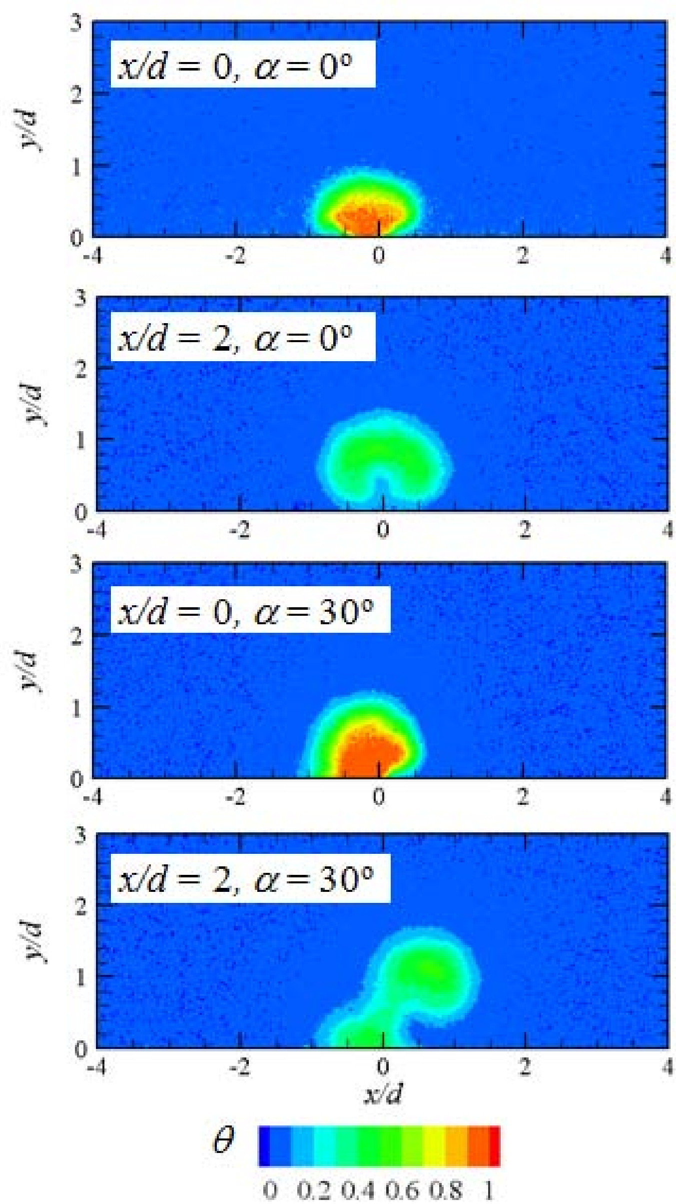

Figure 15 Cross section non-dimensional concentration contours (Circular hole, *M* = 1.0)

increasing the swirl number to $\alpha = 30º$, the positive or negative z side of the spread film cooling layer is rolled up by the strong swirling motion in the film cooling jet itself as mentioned above. The bottom figure in Figure 16 clearly shows this fact. Optimized swirl number for shaped film cooling hole can cause the film jet spread out more in spanwise direction and area coverage further downstream of the shaped hole.

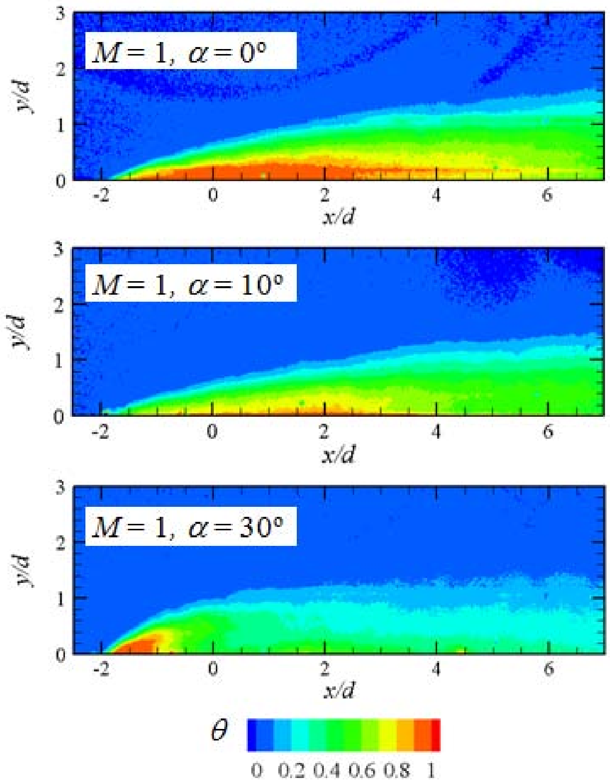

Figure 16 Spatial non-dimensional concentration contours of shaped hole

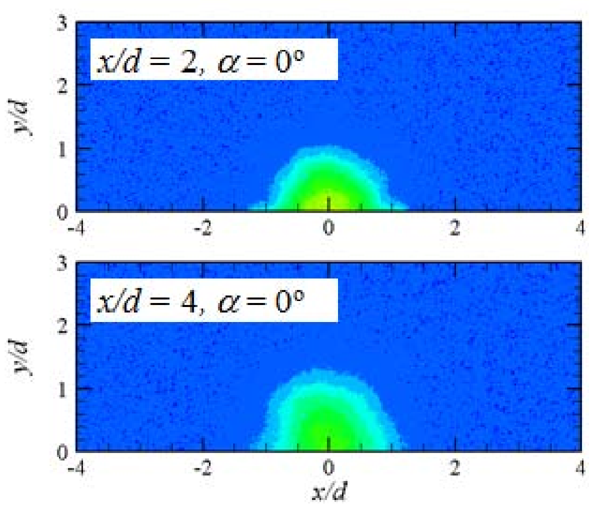

Figure 17.1 Cross section non-dimensional concentration contours (Shaped hole, M = 1.0)

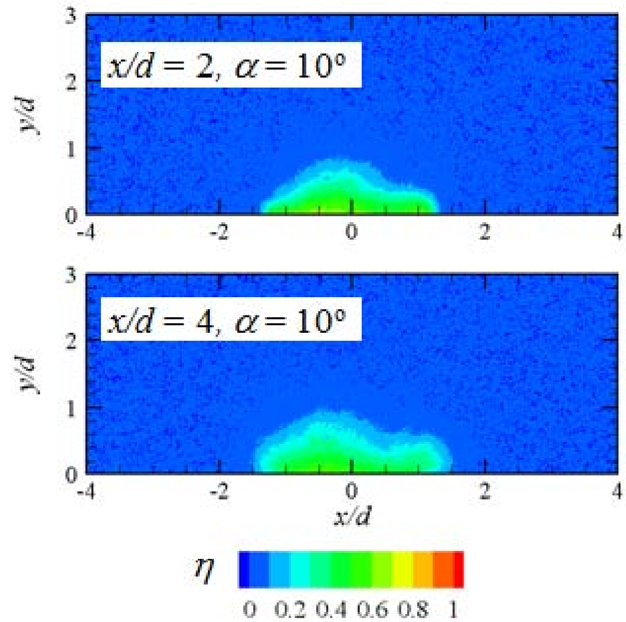

Figure 17.2 Cross section non-dimensional concentration contours (Shaped hole, M = 1.0)

Spatial flow field

Figures 18 and 19 show the time-averaged velocity vectors and vorticity distribution measured for the circular film cooling hole at M = 1.0 by PIV method. The generation of kidney vortex structure is affected by the swirling motion of film cooling flow at $\alpha = 30º$ and film cooling air adheres on the wall. As it is clear from Figure 19, a quite low velocity region and a shear layer was detected behind the circular film cooling hole exit at α = 0º, but penetration of the film cooling jet into

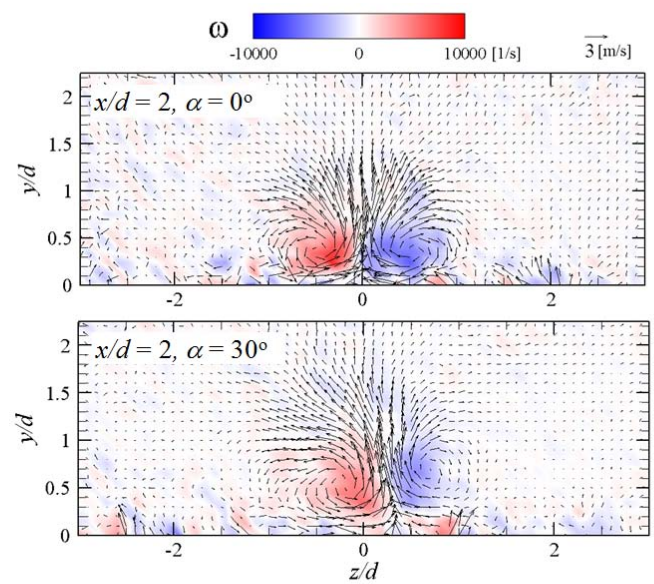

Figure 18 Time-averaged vorticity field of cylindrical film cooling hole at M=1.0

mainstream was suppressed and coolant adhered on the wall at α = 30º. Figures 20 and 21 show the time-averaged vorticity distribution measured for the shaped film cooling hole at M = 1.0 by PIV method. Careful inspection reveals that the jet path on the negative z side wall at α = 30º begins to separate the film cooling layer with increase of impingement nozzle angle α.

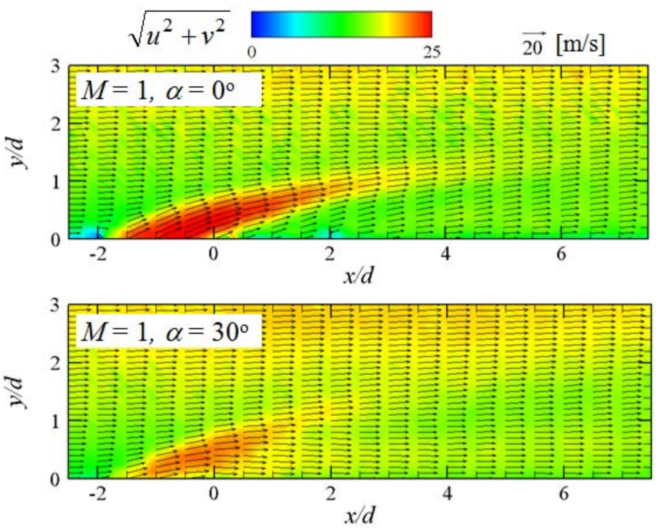

Figure 19 Time-averaged velocity field of circular film cooling hole at M=1.0

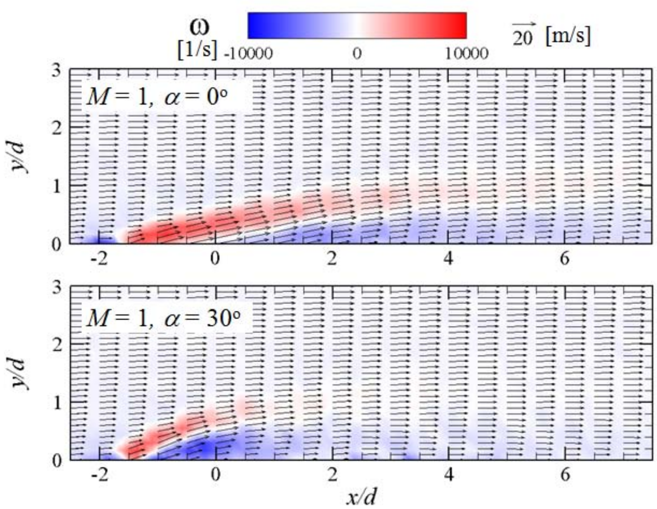

Figure 20 Time-averaged vorticity field of shaped film cooling hole at z/d=0 section

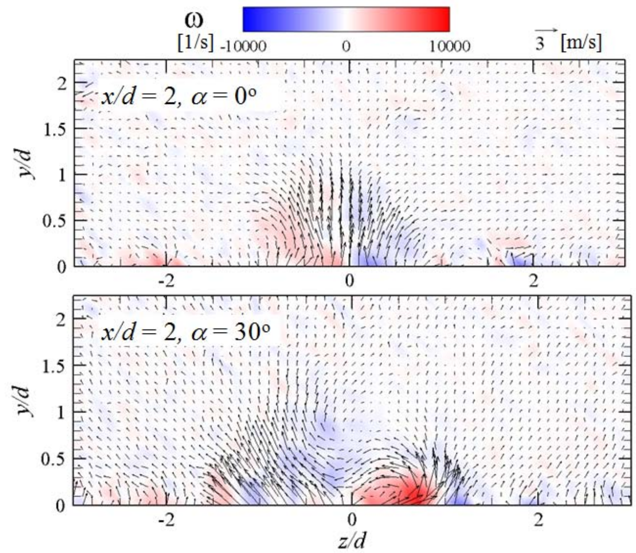

Figure 21 Time-averaged vorticity field of shaped film cooling hole at M=1.0

CONCLUSIONS

The experimental investigation on the effects of swirling motion of film cooling flow on the film cooling effectiveness for a circular and a shaped cooling hole has led to the following conclusions.

1. It appeared by this experimental research work that the swirling film cooling flow applied to a circular film cooling hole decreases the film cooling effectiveness at low swirl number but improve it at high swirl number.

2. The film cooling jet blowing through a circular hole with strong swirling flow improved the film cooling effectiveness. This improvement was attained by the interaction between swirling film jet and mainstream, and the swirling motion destructed the kidney vortex structure and made the film cooling air adhere on the wall.

3. Application of the swirling flow with low swirl number to a shaped film cooling is also effective to improve the film cooling effectiveness. The film cooling effectiveness shows the maximum value at α = 10º among the four cases at α = 0º, 10º, 20º and 30º. Thus, it is estimated that there is an optimum combination between a shaped hole geometry and impingement nozzle angle α. These results can be applied to the cooling design of blades and vanes.

4. The swirling motion in the film cooling flow sometime deteriorates the film cooling effectiveness and we must reflect these facts to the design of actual turbine nozzle vane and blade, and must study the internal flow effect on film cooling from stand point of view of film cooling with swirl coolant.

NOMENCLATURE

a thermal diffusivity
C concentration
D diffusion factor
d film hole diameter
G_a angular momentum mass flow rate
G_t translation momentum mass flow rate
I emission intensity
Le Lewis number
M blowing ratio
R radius
r distance from center point
S swirl number
Sc Schmidt number
T temperature
u, v, w velocity
x, y, z coordinate system

Greek

α impingement jet angle
θ non-dimensional concentration
η film cooling effectiveness
ρ density
ω angular velocity

Subscript

a air
aw adiabatic wall
c coolant
f film
w wall
∞ mainstream

ACKNOWLEDGMENTS

The authors would like to express grateful acknowledgments to the sustained support of Mitsubishi Heavy Industries Ltd., during the course of this research.

REFERENCES

[1] Goldstein, R. J., 1971, "Film Cooling", *Advances in Heat Transfer*, Vol. 7, pp. 321-379.
[2] Bogard, D. G. and Thole, K. A., 2006, "Gas Turbine Film Cooling", *J. of Propulsion and Power,* 22, pp. 249–270.
[3] Eriksen, V, L. and Goldstein, R. J., 1974, "Heat Transfer and Film Cooling Following Injection Through Inclined Circular Tubes", *J. of Heat Transfer*, pp. 239-245.
[4] Bernsdorf, S., Rose, M. G. and Abhari, R. S., 2005, "Modeling of Film Cooling - Part I: Experimental Study of Flow Structure", *ASME Paper No. GT2005-68783*.
[5] Goldstein, R. J. and Eckert, E. R. G., 1994, "Effect of hole geometry and density on three-dimensional film cooling", *Int. J. Heat and Mass Transfer*, 17, pp. 595-607.
[6] Bell, C. M., Hamakawa, H. and Ligrani, P. M., 2000, "Film Cooling From Shaped Holes", *J. of Turbomachinery*, 122, pp. 224-232.
[7] Takeishi, K., and Aoki, S., 2001, "Contribution of Heat Transfer to Turbine Blades and Vanes for High Temperature Industrial Gas Turbines: Part 1, Film Cooling", *Ann. N. Y. Acad. Sci.*, Vol. 934, pp. 305-312.
[8] Yu, Y, Yen, C. -H. Shin, T. I. -P. and Chyu, M. K. 2000, "Film Cooling Effectiveness and Heat Transfer Coefficient Distribution Around Diffusion Shaped Holes", *J. of Heat Transfer,* 124, pp. 820-827.
[9] Bunker, R. S., 2005, "A Review of Shaped Hole Turbine Film-Cooling Technology", *J. of Heat Transfer*, 127, pp. 441-453.
[10] Kusterer, K., et al., 2009, "A parametric study on the influence of the lateral ejection angle of double-jet holes on the film cooling effectiveness for high blowing ratios", *ASME Paper GT2009-59321*.
[11] Heidmann, J. D. and Ekkad, S., 2007, "A novel anti-vortex turbine film- cooling hole concept", *ASME paper, GT2007-27528*.
[12] Rigby, D., Heidmann, J. 2008, "Improved Film Cooling Effectiveness by Placing a Vortex Generator Downstream of Each Hole", *ASME Paper GT-2008-51361*.
[13] Ely, M., J., Jubran B., A., 2008, "A Numerical Study on Increasing Film Cooling Effectiveness Through the Use of Sister Holes", *ASME Paper GT-2008-50366*.
[14] Kissel, H. P., Weigand, B., Wolfersdort, J. von, Neumann, S. O. and Ungewickell, A., 2007, "An Experimental and Numerical Investigation of the Effect of Cooling Channel Crossflow on Film Cooling Performance", *ASME Paper GT-2007-27102*.
[15] Kuya, Y., Nuntadusit, C., Ishida, H., Momose, K. and Kimoto, H., 2004, "An Application of Swirling Jet to Film Cooling", *Proc., JSME Thermal Engineering Conference,* Sendai, No.04-28, (in Japanese).
[16] Takeishi, K., Kitamura, T., Komiyama, M., Oda, Y. and Mori, S., 2009, "Study on the thermal and flow fields of shaped film cooling holes", *Int. Symp. on Heat Transfer in Gas Turbine Systems*, Antalya, Turkey,.
[17] Lazano, A., Yip, B. and Hanson, R. K., 1992, "Acetone: a tracer for concentration measurements in gaseous flows by planer laser-induced fluorescence", *Experiments in Fluids,* Vol. 13, 369-376.
[18] Eckert, E. R. G., Sakamoto, H., and Simon, T. W., 2001 "The heat/mass transfer analogy factor Nu/Sh, for boundary layers on turbine blade profiles" *International Journal of Heat and Mass Transfer*, 44, pp.1223-1233.
[19] Kumagai, K., Takeishi, K., Komiyama, M. and Tokunaga, D., 2006, "Numerical and experimental research on a mixing process of film cooling air with mainstream", *Proc., Inter. Heat Transfer Conference*, No. FCV-14.
[20] Kajiuchi, T., Takeishi, K., Oda, Y., and Kumagai, T., 2007, "Numerical and Experimental Research on the Film Cooling Flow Fields from Circular and Shaped Holes", *Proc., Inter. GT Congress*, Paper No. IGTC7 Tokyo TS-109.
[21] Takeishi, K., Oda, Y., Egawa, Y. and Kitamura, T., 2010 "Film Cooling with Swirling Coolant Flow", *WIT Transactions on Engineering Sciences*, 68, pp.189-200.

